Journal of Electronic Materials (2023) 52:1250–1257
https://doi.org/10.1007/s11664-022-10073-3

ORIGINAL RESEARCH ARTICLE

Magnesium Bis(Oxalate)Borate as a Potential Electrolyte for Rechargeable Magnesium Ion Batteries

Jesús Guzmán-Torres[1] · Dalmy L. Ochoa-Gamboa[1] · Lorena L. Garza-Tovar[1] · Luis C. Torres-González[1] · Salomé M. de la Parra-Arciniega[1] · Edgar González-Juárez[1] · Idalia Gómez[1] · Eduardo M. Sánchez[1]

Received: 11 July 2022 / Accepted: 3 November 2022 / Published online: 28 November 2022
© The Minerals, Metals & Materials Society 2022

Abstract

Magnesium bis(oxalate)borate salt ($Mg(B(C_2O_4)_2)_2$ or $Mg(BOB)_2$) was prepared by a solid-state reaction solvent-free process, and is potentially viable to be used as an electrolytic material for magnesium ion batteries (MIBs). The synthesis was achieved by mixing oxalic acid, boric acid, and magnesium hydroxide using a molar ratio of 4:2:1, respectively. The resulting powders were dried under vacuum at 60°C, then pressed into pellets, and heated at 110 °C for 3 h, with a final heating at 150 °C for 12 h. The crystalline structure and particle morphology of the reaction product were characterized by x-ray diffraction (XRD) and scanning electron microscopy (SEM). Fourier-transform infrared (FTIR) spectroscopy results confirmed the presence of functional groups in the final product, identified by the absorption bands C = O, C-O-B-O-C, O-B-O, and B-O. In order to evaluate the electrochemical properties, pure crystalline $Mg(BOB)_2$ powders were dissolved in tetrahydrofuran (THF) and evaluated within a three-electrode electrolytic cell and in half-cells through cyclic voltammetry (CV) curves.

Keywords MIBs · $Mg(BOB)_2$ · electrolyte · Mg stripping/plating

Introduction

Technological developments associated with the needs of electronic devices with high performance and portability have stimulated research alongside the enhancements of new forms of energy storage and supply.[1] The improvement of energy storage devices will allow the achieving of the most important current challenges, namely, the reduction of our dependence on fossil fuels through the development of advanced materials that can efficiently store electricity from renewable energy sources.[2]

In recent decades, several research groups have intensified the search for alternative energy sources, from solar, wind, hydraulic, nuclear, or chemical energies. Rechargeable batteries are based on chemical energy.[3] Nowadays, lithium ion batteries (LIBs) are the most capable energy storage devices. However, lithium has limited abundance.[4]

On the other hand, the cost for the extraction and manufacture of lithium and sodium are more expensive than that for magnesium (Mg); magnesium is a sustainable alternative to stop the excessive consumption of lithium.[5] Another advantage of the use of magnesium over lithium is the lack of dendrite growth, which has a positive impact on battery performance; nevertheless, one of the disadvantages corresponds to the short-term loss of storage capacity once the battery is partially discharged.[6] Although magnesium offers a great potential for low-cost and safe energy storage devices, rechargeable magnesium ion batteries (MIBs) are currently at the research stage.[7]

Recently developed MIBs are still far from competitive with lithium batteries, in terms of output voltage and energy density.[8] The design of novel electrolytic materials could offer the potential to provide high-purity magnesium anodes as well as good compatibility.[9] Likewise, a highly conductive electrolyte is of main importance for a high-rate battery performance, with, furthermore, the need to avoid unstable flammable electrolytes such as those relying on ether solvents. One of the main challenges in MIBs is the inferior electrochemical performance compared to LIBs, because magnesium cyclability is difficult to achieve in most electrolytes.[10–12]

✉ Eduardo M. Sánchez
eduardo.sanchezcv@uanl.edu.mx

[1] Facultad de Ciencias Químicas, Universidad Autónoma de Nuevo León, Av. Universidad S/N Ciudad Universitaria, C.P. 66451 San Nicolas de los Garza, Nuevo León, México

In this work, magnesium bis(oxalate)borate, $Mg(BOB)_2$ was prepared by a low-temperature solid-state synthesis route. The $Mg(BOB)_2$ was dissolved in various solvents and evaluated as an electrolyte. It was found that magnesium salt has a high solubility in tetrahydrofuran (THF), and that this mixture allowed Mg stripping/plating on the surface of a platinum working electrode when cycled electrochemically in three-electrode cells, showing electrochemical characteristics for a potential application in MIBs, as well as in other energy storage and conversion devices.

Experimental

Synthesis of $Mg(BOB)_2$

$Mg(BOB)_2$ was synthesized using magnesium hydroxide, $Mg(OH)_2$, (reagent grade ≥ 95%; Sigma-Aldrich), boric acid, H_3BO_3, (ACS reagent ≥ 99.5%; Sigma-Aldrich), and oxalic acid, $C_2H_2O_4$, (anhydrous ≥ 99%; Sigma-Aldrich) as starting materials (Table I). Stoichiometric amounts were weighed and mixed into the reaction pathway as:

$$4C_2H_2O_4 + 2H_3BO_3 + Mg(OH)_2 \rightarrow Mg(BOB)_2 + 8H_2O \quad (1)$$

The reaction was carried out by a low-temperature solid-state method, the first step consisting of drying all the precursors inside a vacuum oven at 60°C for 1 h, and subsequently mixing them for 15 min within an agate mortar and preparing dry-pressed pellets by applying a pressure of 2 MPa (gauge pressure). The homogeneous mixture was compressed into various cylindrical pieces with an area of 1.3 cm^2 and a thickness of 0.5 cm. Afterwards, the pellets were initially heat-treated at 110 °C for 3 h, to remove residual water, then a subsequent heat treatment at 150 °C for 12 h was carried out, thus obtaining $Mg(BOB)_2$ salt. The reaction product was transferred inside an argon-filled (O_2 and H_2O < 1 ppm) glove box (Omni-Lab 0210; VAC) as rapidly as possible, avoiding exposure to ambient atmosphere, then the pellets were ground before analysis.

Acetonitrile (ACN), propylene carbonate (PC), ethylene carbonate (EC), dimethyl carbonate (DMC), and tetrahydrofuran (THF) solvents were purchased from Sigma-Aldrich as battery-grade reagents and employed as received.

Structural and Morphological Characterization

The crystalline structure as well as the phase identification of $Mg(BOB)_2$ were attained through McMaille software, with the results from prior characterization by x-ray diffraction (XRD; D2-Phaser; Bruker) with a CuKα radiation source (λ = 1.5418 Å). Particle size and morphology were analyzed using scanning electron microscopy (SEM; Neoscope JCM-6000; JEOL). Fourier-transform infrared spectroscopy (FTIR; Interspec 200-X) was carried out within the wave number range from 4000 cm^{-1} to 400 cm^{-1}. Potassium bromide (KBr) pellets were used as a calibration blank and holder for sample analysis.

Preparation of Electrolytes

$Mg(BOB)_2$ powder was used without further purification. The electrolytes were prepared at 50 mM concentration in each of the following solvents: ACN, PC, EC:PC (1:1 vol%), EC:PC:DMC (1:1:3 vol%), and THF. Every resulting solution was stirred for 24 h before electrochemical characterization. All the electrolytes based on the $Mg(BOB)_2$ salt were prepared under inert conditions in a glove box. The electrochemical cyclability was evaluated for each electrolyte-prepared targeting to select the best solvent performance.

Electrochemical Measurements

Cyclic voltammetry (CV). Analysis was performed in three-electrode cells with a VMP3 potentiostat/galvanostat (Biologic Science Instruments) at room temperature using a platinum (Pt) working electrode (2 mm diameter; CH Instruments), and Mg foils (99.9% purity; Sigma-Aldrich) were used as counter and reference electrodes.

Linear scanning voltammetry (LSV). The electrolyte selected for the LSV test was 250 mM $Mg(BOB)_2$/THF, which required several working electrodes (WE), such as copper (Cu), silver (Ag) plated with gold (Ag/Au), silver, glassy carbon (GC), stainless steel 304 (SS304), nickel (Ni), stainless steel 316 (SS316), Pt, and aluminum (Al). Mg foils were used as counter and reference electrodes.

Electrochemical impedance spectroscopy (EIS). The ionic conductivity of various electrolytes was studied by EIS. Glass-fiber membranes were soaked with 120 µL of the electrolyte with different concentrations, *C*, of $Mg(BOB)_2$/THF,

Table I Raw materials as $Mg(BOB)_2$ precursors

Compounds	Molecular weight	Chemical formula	Purity
Oxalic acid	90.03 g/mol	$C_2H_2O_4$	Anhydrous, ≥ 99.0%
Boric acid	61.83 g/mol	H_3BO_3	ACS reagent, ≥ 99.5%
Magnesium hydroxide	58.32 g/mol	$Mg(OH)_2$	Reagent grade, ≥ 95%

where C = 50 mM, 100 mM, 150 mM, 200 mM, 250 mM, 300 mM, 350 mM, and 400 mM. The membranes were then placed between a pair of SS316 blocking electrodes inside a CR2032 coin cell. The cells were conditioned through heating at 40 ºC for 12 h to obtain good contacts between the electrolytes and electrodes, then the cells were slowly cooled to room temperature and rested for 24 h before being tested on electrochemical workstations. EIS measurements were carried out in the temperature range of 30–80 °C, and every cell was allowed to reach thermal equilibrium for at least 3 h prior to each measurement. EIS curves were recorded in the frequency range from 1000 Hz to 10 mHz, applying a sinusoidal wave with an amplitude of 10 mV, as published elsewhere.[13]

The ionic conductivity values were calculated from Eq.2, where σ is the ionic conductivity, l is the thickness of the electrolyte-soaked glass-fiber membrane, S is the cross-section area of the glass fiber membrane, and R represents the resistance determined by the Nyquist plot (see Figure S1 in the supplementary information):

$$\sigma = \frac{l}{SR} \tag{2}$$

Results and Discussion

Synthesis and Characterization of $Mg(BOB)_2$

Figure 1 shows the results obtained by XRD of $Mg(BOB)_2$ (see Figure S2 that include the XRD pattern of the precursors and reaction product). Using McMaille software for power diffraction pattern indexing[14] via Expo2014 [https://www.ba.ic.cnr.it/softwareic/expo/], we were able to determine the structure cell parameters of $Mg(BOB)_2$ as a monoclinic structure belonging to the P21/c space group, with a = 11.63 Å, b = 10.16 Å, c = 8.80 Å, α = γ = 90°, and β = 94.02°, a cell volume of 1039.29 $Å^3$ and Z = 2 formulae per unit cell. The average size of the crystallites was determined from the four highest intensity peaks, employing Scherrer's equation (Eq. 3), where D is the crystal grain size, m is the full width at half-maximum (FWHM), λ is the wavelength of the x-rays, θ is the diffraction angle, and K is the Scherrer constant, expressed in radians with K = 0.89.

$$D = \frac{K\lambda}{m\cos\theta} \tag{3}$$

Furthermore, the value of the FWHM should also be expressed in radians to ensure unit consistency throughout the calculation process.[15] The crystallite sizes of the five maximum intensities are presented in Table II. Based on the FWHM value obtained from the XRD pattern, it was found that the average size of the crystallites was 44.89 nm, with a maximum size of 54.15 nm and a minimum size of 35.47 nm. The morphology of $Mg(BOB)_2$, observed in the inset in Fig. 1, was obtained through SEM. Irregular microparticles with a size in the range of micrometers can be seen, similar to research reported in the literature.[16–23]

The FTIR spectrum of the synthesized $Mg(BOB)_2$ is shown in Fig. 2, This technique allows the identification of functional groups with the powder technique[24] (see Figure S3 showing the FTIR spectrum of the precursors and the reaction product). The main infrared peaks of $Mg(BOB)_2$ and their functional group characteristic bands are shown in Table III. The vibration peaks at wavenumbers 3446 and 3215 cm^{-1} corresponding to the O-H bonds are attributed to water absorbed by the particles.[25] In turn, the bands observed at 2673 and 2256 cm^{-1} can be associated to stretch vibrations of the atoms in the C–O bond[26] from gaseous CO_2 absorbed in the analyzed powders. Absorption bands at 1824 and 1791 cm^{-1} indicate the presence of functional groups C = O with oscillations in and out of phase from BOB anions,[27] respectively. Asymmetric and symmetric stretch COO were ascribed to wavenumbers at 1650 and 1456 cm^{-1}, respectively.[28]

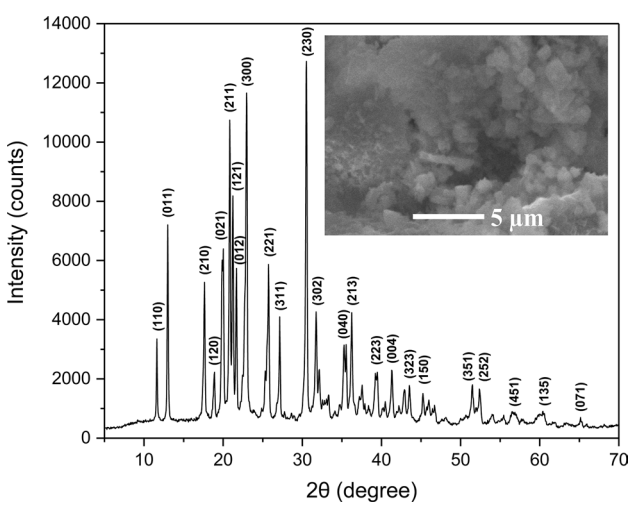

Fig. 1 XRD pattern of $Mg(BOB)_2$; inset SEM image of the solid.

Table II Crystallite size calculation results by Scherrer's equation

2θ (degree)	FWHM (radians)	Crystallite size (nm)
12.97	0.146	54.155
20.81	0.168	47.544
21.22	0.168	47.575
22.95	0.226	35.470
30.49	0.205	39.720

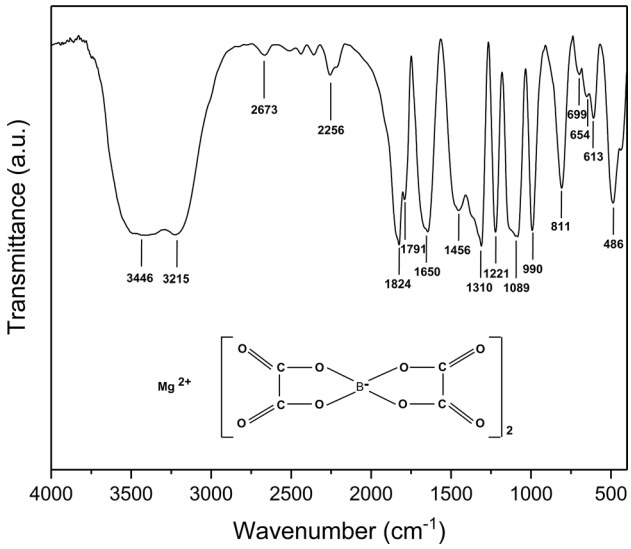

Fig. 2 FTIR spectrum of $Mg(BOB)_2$; inset structure of the molecule.

Table III Absorption bands in $Mg(BOB)_2$

Functional groups	Wavenumber (cm^{-1})
O-H	3446, 3215
C-O	2673, 2256
C = O oscillate in phase	1824
C = O oscillate out of phase	1791
COO^- asymmetric stretch	1650
COO^- symmetric stretch	1456
C-O-B-O-C stretch	1310
C-O-C asymmetric stretch	1221
O-B-O symmetric stretch	1089
C-O-C symmetric stretch	990
O-B-O symmetric	811
O-B-O asymmetric stretch	699
COO^- deformation	654
B-O deformation	613
BO_4	486

Fingerprint bands of $Mg(BOB)_2$ salt are present at 1310, 1221, 1089, and 990 cm^{-1}, which represent the C-O-B-O-C stretch, C-O-C asymmetric stretch, and the O-B-O and C-O-C symmetric stretches, respectively. Further, other absorption bands of O-B-O symmetric and O-B-O asymmetric stretches show at wavenumbers 811 and 699 cm^{-1}, as well as the BO_4 functional group at 486 cm^{-1}, comparably to the FTIR spectra reported in the literature.[29] The wavenumbers 654 and 613 cm^{-1} are typical peaks of COO^- and B-O deformations, respectively.[20]

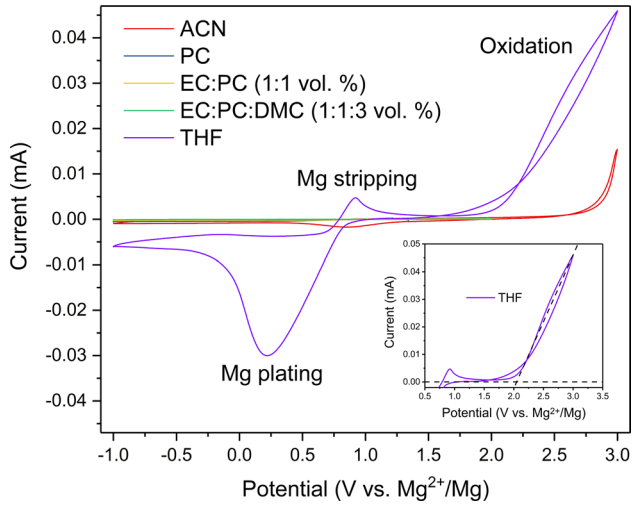

Fig. 3 CV results of Mg stripping/plating containing 50 mM $Mg(BOB)_2$ dissolved in different solvents collected at a scan rate of 25 mV s^{-1} within the potential range from − 1.0 to 3.0 V versus Mg^{2+}/Mg; inset zoom at 0.9 V to observe Mg stripping, and oxidation of the electrolyte in the first cycle (dashed line).

Electrochemical Properties of $Mg(BOB)_2$ in Different Solvents

The solubility of $Mg(BOB)_2$ was evaluated in different solvents, CV tests were performed via a low concentration of about 50 mM $Mg(BOB)_2$ in several solvents, at an experimental scan rate of 25 mV s^{-1} within the potential range − 1.0–3.0 V (vs. Mg^{2+}/Mg). As can be observed in Fig. 3 (see also Figure S4 showing the CV curves using different solvents), the amount of magnesium salt dissolved in the PC (blue graph), EC:PC (1:1 vol%, yellow graph), and EC:PC:DMC (1:1:3 vol%, green graph) solvents showed null Mg stripping/plating. This behavior can be attributed to these solvents being of organic carbonate type, hence considered unsuitable for Mg electrolytes, since cathodic decomposition forming a passivation layer occurred[30] as observed to occur in Pt WE. In addition, those solvents represents a serious risk for safety in batteries, being highly volatile and flammable, which prevent compliance with the highest safety standards for the immediate applications required.[31] Moreover, the use of ACN as a solvent showed Mg plating but not Mg stripping. Although it can function as an electron donor ligand, studies based on Mg electrolytes using ACN reported contradictory results.

One study has reported the formation of a thick passivation layer on a Mg-coated electrode when working at high overpotential with electrolytes containing Mg salt/ACN.[32] Nevertheless, another study has revealed ACN decomposition at a cathodic potential, with a simultaneous reduction in the current of Mg plating, owing to a reduction potential

in the ACN that is closer to Mg^{2+}/Mg (2.5 V and 2.3 V, respectively).[33]

In general, the use of ACN as a solvent for Mg electrolytes remains a challenge to understand, as well as the rest of the solvents. We conclude that the high insolubility of magnesium salts[34–36] cannot be improved, even by increasing the solvent amounts. Therefore, the coordination of specific anions is more strongly controlled by the solvent structure instead of by the salt concentration in the range from 100 to 500 mM. Meanwhile, the solvation tendency of multivalent cations in these types of solvents provides information on the structural relationships, promoting the design and research to develop better electrolytes.[37] Regarding the THF solvent, it was the only one displaying Mg plating at − 0.03 mA, and Mg was stripping at 0.005 mA of current. In this sense, THF was selected as the best solvent due to its high compatibility with $Mg(BOB)_2$, similar to the type of salts in previous reports.[38–40] When analyzing the electrolyte containing 50 mM $Mg(BOB)_2$/THF, a decomposition was observed above 2 V, as can be seen in the inset in Fig. 3. This finding allowed us to modify the working potential window at this voltage for the subsequent cyclability tests with different concentrations of the $Mg(BOB)_2$/THF electrolyte.

Electrochemical Behavior of $Mg(BOB)_2$ in THF at Different Cycles

The electrolyte with a concentration of 250 mM $Mg(BOB)_2$/THF was selected for its high current densities (*J*), and evaluated in three-electrode cells by means of CV curves up to 250 cycles, as can be seen in Fig. 4 (see Figure S5 and Table S1 in supplementary information). Starting from an initial open circuit voltage (OCV) of 1.10 V (inset a in Fig. 4) until reaching a final OCV ≈ 1.3 V after 250 cycles. The cyclability started in the cathodic zone, and, for the first cycle, the highest amount of cathodic charge current density (Mg plating) of about $J \approx$ -1.74 mA cm^{-2} was obtained (inset b in Fig. 4), as well as an anodic charge current density of $J \approx 0.40$ mA cm^{-2} (Mg stripping) related to other concentrations (see Table S1). For the tenth cycle, the same amount of *J* was obtained in the Mg plating; however, this was not the case for the *J* in the Mg stripping process, since its original value decreased by up to 50%.

For cycle number 50 ($J \approx -1.46$ mA cm^{-2} in Mg plating) and cycle number 100 ($J \approx -1.34$ mA cm^{-2} in Mg plating), the change in the amount of anodic charge current density was not greater than 0.02 mA cm^{-2}, the value of *J* was about 0.11 mA cm^{-2} and remained constant for cycles 150, 200, and 250, whereas the values of *J* were only reflected in the Mg plating. There was a gradual drop to $J \approx -1.14$ mA cm^{-2} in the Mg plating after 250 cycles, resulting in highly competitive values, compared with those reported in the literature for Mg salts based on borates with cathodic

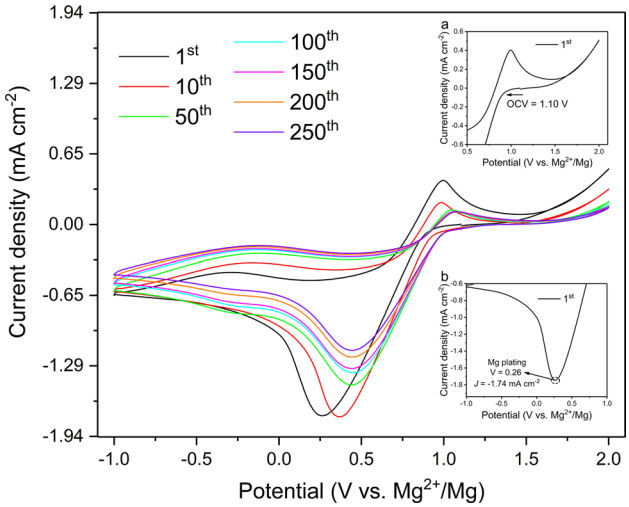

Fig. 4 CV results of the Mg stripping/plating process containing 250 mM $Mg(BOB)_2$ dissolved in THF, collected at a scan rate of 25 mV s^{-1} within the potential range of − 1.0 to 2.0 V versus Mg^{2+}/Mg; insets a zoom at 0.9 V to observe Mg stripping, and b zoom at 0.3 V to observe Mg plating in the first cycle.

charge currents of around ≈ 0.03 mA,[13] offering a broad opening to a field of research to explore the performance of these novel electrolytes at high temperatures and with different solvents.

The three-electrode cells cycling up to 250 cycles (250 mM/THF) in the present work displayed a good cyclability performance from start to finish, compared to the other concentrations studied (see Figure S5 in supplementary information), showing excellent Mg stripping/plating, denoting a high reversibility, the principal characteristic of which is fundamental in electrolytes for secondary magnesium batteries.[41]

Anodic Stability of $Mg(BOB)_2$ in THF

The LSV test results can be seen in Fig. 5. In a new electrolyte at the same molar concentration (250 mM/THF), different WE were compared with the objective of evaluating their anodic stability. It was found that Cu WE generated lower electrochemical stability (1.05 V vs. Mg^{2+}/Mg), and that Al WE offered the highest electrochemical stability (3.5 V vs. Mg^{2+}/Mg), typically the most used materials as current collectors for commercial batteries.[42]

In order to evaluate the difference between most used current collectors for MIBs, two alloys, SS316 and SS304, were included in the LSV measurements. It was determined that SS316 achieved a better electrochemical stability. In the same way, this material has been reported to display a lower steel corrosion,[43] whereas in this work, the material managed to reach a slightly higher value of ≈ 0.5 V above SS304, therefore, for the application in MIBs, contributing

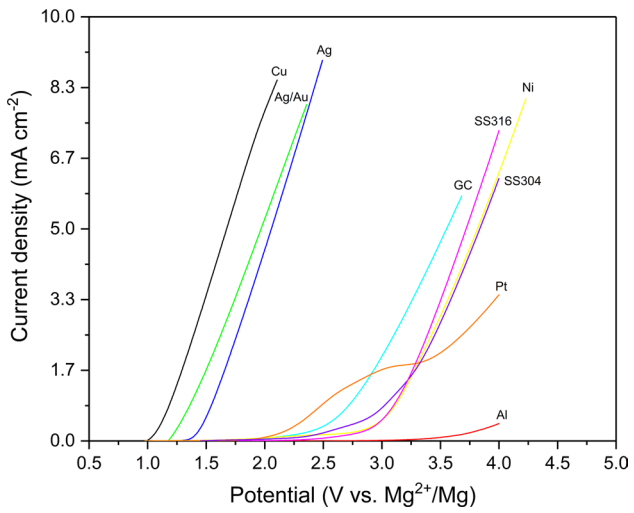

Fig. 5 LSV curves of the 250 mM $Mg(BOB)_2$/THF electrolyte collected at a scan rate of 25 mV s^{-1}. Cu (black), Ag/Au (green), Ag (blue), Pt (orange), GC (turquoise), SS304 (purple), SS316 (fuchsia), Ni (yellow), and Al (red) WE and Mg foils were used as counter/reference electrodes (Color figure online).

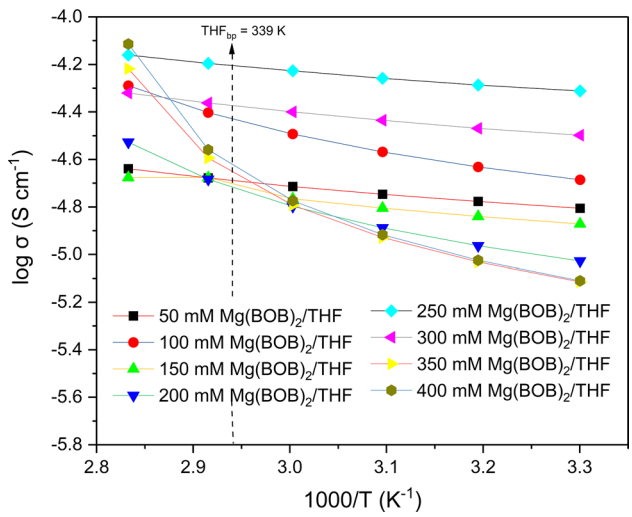

Fig. 6 Arrhenius plot of the ionic conductivity in different electrolyte of *C* $Mg(BOB)_2$/THF concentration, where *C* = 50 mM, 100 mM, 150 mM, 200 mM, 250 mM, 300 mM, 350 mM, and 400 mM; lines are just guides to the eye; the THF boiling point is 339 K.

positively to employing a broad potential window, as this improvement will currently support the development of new materials.[44]

Otherwise, Ag and Ag/Au WE did not reach a potential beyond 2 V, since the electrolyte rapidly decomposed, so these results were not beneficial for its application in MIBs. Thus, GC, Ni, and Pt WE were able to withstand a voltage similar to an electroactive magnesium salt, as reported.[45]

For the preparation of prototype half-cells, we recommend using SS316 current collectors. We were able to verify in this work that three-electrode cells showed a good anodic stability of 2.8 V versus Mg^{2+}/Mg, in accordance with previously reported research, employing CR2032 coin cell type SS316 in Mg^{2+}/Li^{+} hybrid-ion batteries, with a suitable performance.[46]

Ionic Conductivity of $Mg(BOB)_2$ in THF

Finally, the electrolytes were evaluated with the blocking electrode technique, using a CR2032 coin cell SS316 to measure its conductivity at different temperatures. As shown in Fig. 6, the ionic conductivities exhibited a linear behavior according to the Arrhenius equation (Eq. 2). In addition to this, the electrolyte with the concentration of 250 mM/THF again presented the best results at room temperature, as well as in the cyclability tests, achieving an ionic conductivity value of 4.9×10^{-5} S cm^{-1}, remaining above a superior performance compared with the other combinations.

Likewise, the electrolyte with the concentration of 400 mM $Mg(BOB)_2$/THF, which did not present good electrochemical properties in the cyclability measurements, showed an increase in conductivity with a value of about 7.9×10^{-5} S cm^{-1} at 80 °C, these results confirming that Mg electrolytes can withstand higher operating temperatures (see Figure S6 for results in half-cells at room temperature), thus improving its experimental specific capacities,[47] similar to solid polymer electrolytes, which demonstrates a high dependency with temperature to improve efficiency in the batteries.[41] Consequently, the 250-mM $Mg(BOB)_2$ electrolyte has the potential to be further explored, as, in ionic conductivity values, it only displays one order of magnitude lower than its analog.[48] The change in the curve slopes in Fig. 6 can be associated with the boiling point of the THF solvent.

Conclusions

A magnesium salt $Mg(BOB)_2$ was obtained using oxalic acid, boric acid, and magnesium hydroxide as a low-cost and high-purity anhydrous raw material by applying solid-state synthesis. A Mg-based electrolyte prepared with 250 mM $Mg(BOB)_2$/THF has a highly reversible Mg cycle behavior (> 250 cycles), a wide anodic stability (2.8 V vs. Mg^{2+}/Mg), and a good ionic conductivity at room temperature (4.9×10^{-5} S cm^{-1}). The electrolyte had good chemical and electrochemical properties, such as low toxicity, low volatility, once the devices were assembled, and high reversibility, when being evaluated in three-electrode cells and in half-cells, assuming the challenges of the complex interactions of the electrolyte $Mg(BOB)_2$/THF with the different solvents studied, as well as with the prepared commercial

electrodes. Therefore, more work is required to prove its full potential as a high-performance electrolyte for MIBs.

Supplementary Information The online version contains supplementary material available at https://doi.org/10.1007/s11664-022-10073-3.

Acknowledgments Authors would like to Facultad de Ciencias Químicas, Universidad Autónoma de Nuevo León for financial support and the laboratory equipment used in this project (Materials Laboratory 2) at División de Estudios de Posgrado. Jesús Guzmán-Torres also thanks to CONACYT for the scholarship awarded to continue the PhD studies.

Author Contributions JG-T: Investigation, validation, software, formal analysis, and writing-original draft. DLO-G: Helped with electrolytes preparation. LLG-T: XRD testing participation. LCT-G: Electrochemical testing participation. SM de la P-A: FTIR testing participation. EG-J: Battery assembly supervision. IG: Conceptualization and writing comments. EMS: Conceptualization, supervision, writing-review and editing, funding acquisition. All authors read and approved the final manuscript.

Funding Consejo Nacional de Ciencia y Tecnología,888794,Jesus Guzman-Torres,Universidad Autónoma de Nuevo León,1940246

Conflict of interest The authors declare no conflict of interest.

References

1. Y. Liang, C.-Z. Zhao, H. Yuan, Y. Chen, W. Zhang, J.-Q. Huang, Yu. Dingshan, Y. Liu, M.-M. Titirici, Y.-L. Chueh, Yu. Haijun, and Q. Zhang, A review of rechargeable batteries for portable electronic devices. *InfoMat* 1, 6 (2019).
2. D. Gielen, F. Boshell, D. Saygin, M.D. Bazilian, N. Wagner, and R. Gorini, The role of renewable energy in the global energy transformation. *Energy Strategy Rev.* 24, 38 (2019).
3. B. John, Goodenough, How we made the Li-ion rechargeable battery. *Nat. Electron.* 1, 204 (2018).
4. A. Ramar and F.-M. Wang, Advances in polymer electrode materials for alkali metals (lithium, sodium and potassium)-ion rechargeable batteries. *J. Mater. Sci. Mater.* 31, 21832 (2020).
5. A. Watanabe, K. Yamamoto, Y. Orikasa, T. Masese, T. Mori, T. Uchiyama, T. Matsunaga, and Y. Uchimoto, Reaction mechanism of electrochemical insertion/extraction of magnesium ions in olivine-type $FePO_4$. *Solid State Ion.* 349, 115311 (2020).
6. X. Lei, Y. Zheng, F. Zhang, Y. Wang, and Y. Tang, Highly stable magnesium-ion-based dual-ion batteries based on insoluble small-molecule organic anode material. *Energy Storage Mater.* 30, 34 (2020).
7. Z. Zhang, S. Dong, Z. Cui, Du. Aobing, G. Li, and G. Cui, Rechargeable magnesium batteries using conversion-type cathodes: a perspective and minireview. *Small Methods* 2, 1800020 (2018).
8. T. Placke, R. Kloepsch, S. Dühnen, and M. Winter, Lithium ion, lithium metal, and alternative rechargeable battery technologies: the odyssey for high energy density. *J. Solid State Electrochem.* 21, 1939 (2017).
9. R. Attias, M. Salama, B. Hirsch, Y. Goffer, and D. Aurbach, Anode-electrolyte interfaces in secondary magnesium batteries. *Joule* 3, 1 (2019).
10. R. Deivanayagam, B.J. Ingram, and R. Shahbazian-Yassar, Progress in development of electrolytes for magnesium batteries. *Energy Storage Mater.* 21, 136 (2019).
11. R. Dominko, J. Bitenc, R. Berthelot, M. Gauthier, G. Pagot, and V. Di Noto, Magnesium batteries: current picture and missing pieces of the puzzle. *J. Power Sour.* 478, 229027 (2020).
12. M. Rashad, M. Asif, Y. Wang, Z. He, and I. Ahmed, Recent advances in electrolytes and cathode materials for magnesium and hybrid-ion batteries. *Energy Storage Mater.* 25, 342 (2020).
13. Z. Zhang, Z. Cui, L. Qiao, J. Guan, Xu. Huimin, PuHu. Xiaogang Wang, Du. Huiping, S. Li, X. Zhou, S. Dong, Z. Liu, G. Cui, and L. Chen, Novel design concepts of efficient Mg-ion Electrolytes Toward High-Performance Magnesium-Selenium And Magnesium-Sulfur Batteries. *Adv. Energy Mater.* 7, 1602055 (2017).
14. A. Le Bail, Monte carlo indexing with McMaille. *Powder Diffr.* 19, 249 (2004).
15. K. He, N. Chen, C. Wang, L. Wei, and J. Chen, Method for determining crystal grain size by X-Ray diffraction. *Cryst. Res. Technol.* 53, 1700157 (2018).
16. E.M. Wigayati, C.R. Ratri, I. Purawiardi, F. Rohman, T. Lestariningsih, Microstructure analysis of synthesized LiBOB. *Indones. J. Chem.* 15, 242 (2015).
17. C. Ge, L. Wang, L. Xue, Wu. Zhong-Shuai, H. Li, Z. Gong, and X.-D. Zhang, Synthesis of novel organic-ligand-doped sodium bis(oxalate)-borate complexes with tailored thermal stability and enhanced ion conductivity for sodium ion batteries. *J. Power Sour.* 248, 77 (2014).
18. L. Wang, W. Han, C. Ge, R. Zhang, Y. Bai, and X. Zhang, Functionalized carboxyl carbon/NaBOB composite as highly conductive electrolyte for sodium ion batteries. *ChemistrySelect* 3, 9293 (2018).
19. T. Lestariningsih, Christin Rina Ratri, Etty Marty Wigayati, and Qolby Sabrina, Characterization of pore and crystal structure of synthesized LiBOB with varying quality of raw materials as electrolyte for lithium-ion battery. *AIP Conf. Proc.* 1711, 060005–060011 (2016).
20. Etty Marti Wigayati, Titik Lestariningsih, Achmad Subhan, Christin Rina Ratri, and Ibrahim Purawiardi, Synthesis and characterization of LiBOB as electrolyte for lithium-ion battery. *Ionics* 22, 43 (2016).
21. Etty Marti Wigayati, Titik Lestariningsih, Christin Rina Ratri, Ibrahim Purawiardi, and Bambang Prihandoko, Synthesis of LiBOB fine powder to increase solubility. *Makara J. Technol.* 21, 26 (2017).
22. C. Zor, Yaprak Subaşı, Durata Haciu, Mehmet Somer, and Semih Afyon, guide to water free lithium Bis(oxalate) borate (LiBOB). *J. Phys. Chem. C.* 125, 11310 (2021).
23. F. Cheng, X. Zhang, Y. Qiu, J. Zhang, Yi. Liu, P. Wei, Ou. Mingyang, S. Sun, Xu. Yue, Q. Li, C. Fang, J. Han, and Y. Huang, Tailoring electrolyte to enable high-rate and super-stable Ni-rich NCM cathode materials for Li-ion batteries. *Nano Energy* 88, 106301 (2021).
24. A.A. Kamnev, A.V. Tugarova, Y.A. Dyatlova, P.A. Tarantilis, O.P. Grigoryeva, A.M. Fainleib, and S. De Luca, Methodological effects in Fourier transform infrared (FTIR) spectroscopy: Implications for structural analyses of biomacromolecular samples. *Spectrochim Acta A Mol. Biomol. Spectrosc.* 193, 558 (2018).
25. E.F. Medvedev and ASh. Komarevskaya, IR Spectroscopic study of the phase composition of boric acid as a component of glass batch. *Glass Ceram.* 64, 42 (2007).
26. K. Nakamoto, *Infrared and Raman Spectra of Inorganic and Coordination Compounds: Theory and Applications in Inorganic Chemistry*, 5th ed., (New York: Wiley, 1997).
27. A. Tsurumaki, M. Branchi, A. Rigano, R. Poiana, and S. Panero, and Maria Assunta Navarra, Bis(oxalato)borate and difluoro(oxalato)borate-based ionic liquids as electrolyte additives to improve the capacity retention in high voltage lithium batteries. *Electrochim. Acta* 315, 17 (2019).

28. T. Lestariningsih, Q. Sabrina, I. Nuroniah, B. Prihandoko, E. Marti Wigayati, and C. Rina Ratri, Study the synthesis of LiBOB compounds using lithium sources from sea water. *J. Phys.: Conf. Ser.* 1282, 012044 (2019).
29. L. Shiyou, L. Wenbo, C. Xiaoling, L. Chunlei, H. Yamin, Y. Li, W. Peng, W. Jie, W. Yuan. Patent number: CN 110305151 A (2019)
30. J. Shi, J. Zhang, J. Guo, and Lu. Jun, Interfaces in rechargeable magnesium batteries. *Nanoscale Horiz.* 5, 1467 (2020).
31. Y. Yamada, J. Wang, S. Ko, E. Watanabe, and A. Yamada, Advances and issues in developing saltconcentrated battery electrolytes. *Nat. Energy* 4, 269 (2019).
32. T. Ichitsubo, T. Adachi, S. Yagi, and T. Doi, Potential positive electrodes for high-voltage magnesium-ion batteries. *J. Mater. Chem.* 21, 11764 (2011).
33. T.T. Tran, W.M. Lamanna, and M.N. Obrovac, Evaluation of $Mg[N(SO_2CF_3)_2]_2$/acetonitrile electrolyte for use in Mg-Ion cells. *J. Electrochem. Soc.* 159, A2005 (2012).
34. J. Muldoon, C.B. Bucur, A.G. Oliver, T. Sugimoto, M. Matsui, H.S. Kim, G.D. Allred, J. Zajicek, and Y. Kotani, Electrolyte roadblocks to a magnesium rechargeable battery. *Energy Environ. Sci.* 5, 5941 (2012).
35. P. Saha, M.K. Datta, O.I. Velikokhatnyi, A. Manivannan, D. Alman, and P.N. Kumta, Rechargeable magnesium battery: current status and key challenges for the future. *Prog. Mater. Sci.* 66, 1 (2014).
36. R. Mohtadi and F. Mizuno, Magnesium batteries: current state of the art, issues and future perspectives. *Beilstein J. Nanotechnol.* 5, 1291 (2014).
37. K. S. Han, N. T. Hahn, K. R. Zavadil, N. R. Jaegers, Y. Chen, J. Z. Hu, V. Murugesan, and K. T. Mueller (2021). Factors influencing preferential anion interactions during solvation of multivalent cations in ethereal solvents. *J. Phys. Chem. C.* 125 6005
38. Z. Ma, D.R. MacFarlane, and M. Kar, Mg cathode materials and electrolytes for rechargeable Mg batteries: a review. *Batter. Supercaps* 2, 1 (2019).
39. Z. Zhao-Karger and M. Fichtner, Beyond intercalation chemistry for rechargeable Mg batteries: a short review and perspective. *Front. Chem.* 6, 656 (2019).
40. L. Kong, C. Yan, J.-Q. Huang, M.-Q. Zhao, M.-M. Titirici, R. Xiang, and Q. Zhang, A review of advanced energy materials for magnesium– sulfur batteries. *Energy Environ. Mater.* 1, 100 (2018).
41. H. Shuai, Xu. Jing, and K. Huang, Progress in retrospect of electrolytes for secondary magnesium batteries. *Coord. Chem. Rev.* 422, 213478 (2020).
42. A. Chernyaev, J. Partinen, L. Klemettinen, B.P. Wilson, A. Jokilaakso, and M. Lundstrom, The efficiency of scrap Cu and Al current collector materials as reductants in LIB waste leaching. *Hydrometallurgy* 203, 105608 (2021).
43. Y. Youssef, W. El Bestawy, M. Ghazy, M. Shehadeh, and I. Hassan, Investigation of the corrosion behaviour of welded area of austenitic stainless steels under stress. *Int. J. Chem. Eng. Appl.* 9, 135 (2018).
44. Y. Zhang, H. Geng, W. Wei, J. Ma, and L. Chen, and Cheng Chao Li, challenges and recent progress in the design of advanced electrode materials for rechargeable Mg batteries. *Energy Storage Mater.* 20, 118 (2018).
45. O. Tutusaus, R. Mohtadi, T.S. Arthur, F. Mizuno, E.G. Nelson, and Y.V. Sevryugina, An efficient halogen-free electrolyte for use in rechargeable magnesium batteries. *Angew. Chem. Int. Ed.* 54, 7900 (2015).
46. S. M. de la Parraarciniega, E. Gonzálezjuárez, R. A. Hernándezcarrillo, R. Brionesmartínez, R. M. Jiménezbarrera, N. A. Garciagómez, E. M. Sánchez. A Mg^{2+}/Li^{+} hybrid-ion battery based on MoS_2 prepared by solvothermal synthesis with ionic liquid assistance. *J. Mater. Sci. Mater. Electron.* 31 14702 (2020)
47. V. Duffort, X. Sun, and L.F. Nazar, Screening for positive electrodes for magnesium batteries: a protocol for studies at elevated temperatures. *Chem. Commun.* 52, 12458 (2016).
48. A.C. Kucuk, T. Minato, T. Yamanaka, and T. Abe, Effects of LiBOB on salt solubility and BiF_3 electrode electrochemical properties in fluoride shuttle batteries. *J. Mater. Chem. A* 7, 8559–8567 (2019). https://doi.org/10.1039/C8TA10396H.

Publisher's Note Springer Nature remains neutral with regard to jurisdictional claims in published maps and institutional affiliations.

Springer Nature or its licensor (e.g. a society or other partner) holds exclusive rights to this article under a publishing agreement with the author(s) or other rightsholder(s); author self-archiving of the accepted manuscript version of this article is solely governed by the terms of such publishing agreement and applicable law.